Atmospheric Research 156 (2015) 1–13

Contents lists available at ScienceDirect

Atmospheric Research

journal homepage: www.elsevier.com/locate/atmos

Predicting lightning activity in Greece with the Weather Research and Forecasting (WRF) model

Theodore M. Giannaros *, Vassiliki Kotroni, Konstantinos Lagouvardos

National Observatory of Athens, Institute for Environmental Research and Sustainable Development, Vas. Pavlou & Metaxa, 15236 Athens, Greece

ARTICLE INFO

Article history:
Received 14 August 2014
Received in revised form 5 December 2014
Accepted 16 December 2014
Available online 24 December 2014

Keywords:
Lightning prediction
WRF model
ZEUS lightning detection network
Storm parameters
Greece

ABSTRACT

In recent years, significant progress has been made in the development and implementation of parameterizations for the prediction of lightning. In the present study, the commonly used Price and Rind lightning parameterization is evaluated. This parameterization has been recently introduced in the state-of-the-art Weather Research and Forecasting (WRF) model, allowing for the online simulation of lightning activity. The evaluation of the parameterization is conducted for ten different single-day events that took place in Greece during the period of years from 2010 to 2013. Results show that the WRF model could be used for real-time lightning prediction applications, given that the lightning parameterization is properly adapted. In particular, the analysis revealed that model-resolved variables related to the microphysics and thermodynamics are necessary for controlling the parameterization of lightning, which otherwise results to significant overprediction. The total ice content, the maximum vertical velocity and the convective available potential energy were found to be the storm parameters that, when combined together, improve the ability of the model to correctly predict lightning, significantly restricting false alarms. This was further highlighted by separately examining two example case studies, for which the numerical simulations successfully reproduced the spatial and temporal characteristics of lightning activity.

1. Introduction

Lightning prediction has gained increasing attention during the past decade. This is understandable considering that it constitutes a natural hazard with potentially lethal impacts on human life. For instance, Elsom (2000) reported that 3 deaths and more than 50 injuries occur in the United Kingdom every year due to lightning activity, while according to Ashley and Gilson (2009) lightning strikes are responsible for approximately 5000 deaths in the United States during the past 50 years. More recently, Papagiannaki et al. (2013) analyzed impacts of severe weather in Greece, reporting 20 deaths from lightning strikes in the period 2001–2011. However, the growing scientific interest is not just limited to public safety. Knowledge of the distribution of lightning is also important for a broad spectrum of geoscience applications, including the initiation of forest fires (e.g. Drobyshev et al., 2010; Liu et al., 2010; Peterson et al., 2010) and the production of ozone (e.g. Biazar and McNider, 1995; Cooper et al., 2007; Hudman et al., 2007; Pickering et al., 1992; Ryu and Jenkins, 2005; Stockwell et al., 1999).

The inarguable importance of lightning has driven significant advances in the development of parameterizations for the prediction of this natural hazard. Most of the existing parameterizations are formulated on the basis of bulk- or resolved-scale storm parameters that have been found to correlate well with lightning flash rates. As early as in the beginning of the 90s, Price and Rind (1992) reported the development of a lightning parameterization based on cloud-top height (hereafter referred to as PR92). Allen and Pickering (2002) and Allen et al. (2010) parameterized lightning flash rates using the square of deep convective mass flux, while Zhao et al. (2009) and Choi et al. (2005) included the convective available potential energy (CAPE) in their similar parameterizations. Other proxies used

* Corresponding author. Tel.: +30 2108109203.
E-mail address: thgian@noa.gr (T.M. Giannaros).

http://dx.doi.org/10.1016/j.atmosres.2014.12.009
0169-8095/

for the parameterization of lightning include the graupel flux and precipitating ice (McCaul et al., 2009), the ice water path (Petersen et al., 2005), the updraft volume (Deierling and Petersen, 2008) and the maximum vertical velocity (Price and Rind, 1992). A comprehensive overview of the storm parameters most commonly used for parameterizing lightning can be found in Barthe et al. (2010).

An alternative way to tackle lightning activity prediction was adopted by Yair et al. (2010) who introduced a lightning potential index (LPI) in the Weather Research and Forecasting (WRF) model as a measure of the potential for charge generation and separation that leads to lightning. The authors had found that LPI might be a useful parameter for predicting lightning. As a continuation of this work, Lynn et al. (2012) introduced into WRF a new prognostic variable, the potential electrical energy (E_p). This variable was used to predict the occurrence of cloud-to-ground and intra-cloud lightning.

Recently, Wong et al. (2013) introduced the PR92 lightning parameterization in the widely implemented WRF model. As highlighted in their study, Wong et al. (2013) were primarily motivated by the necessity to evaluate PR92 at spatial scales between those commonly applied in global chemistry models and cloud-resolving models, and at temporal scales useful for investigating the chemistry of the upper troposphere. However, the results of their work could also be of particular usefulness for real-time weather forecasting applications. This is particularly true considering that WRF is widely used for supporting operational numerical weather prediction (NWP) activities.

The purpose of the present study is to evaluate the WRF-based PR92 lightning parameterization in terms of its applicability for real-time weather prediction applications. In this context, the lightning parameterization was evaluated on an event-by-event basis. The study area, Greece, and the selected case studies provide a unique opportunity for assessing the performance of the WRF model with regards to lightning prediction and suggesting potential improvements, specifically for supporting operational NWP systems. Indeed, the conducted analysis highlights the necessity to properly adapt PR92 by introducing masking filters that aim to control the parameterization of lightning.

2. Methodology

In the context of the present study, the WRF model, version 3.5.1 (Skamarock et al., 2008), was implemented for 10 selected cases in order to verify its ability in terms of predicting lightning activity in Greece. The implementation of the model was conducted in two stages. At the first stage, several numerical experiments were conducted to assess the model's skill for precipitation forecast, using various combinations of parameterizations for the planetary boundary and surface layer, and microphysics. At the second stage, WRF was implemented using the optimal set of physics schemes in order to evaluate its skill for predicting lightning activity.

2.1. Model setup

Two one-way nested modeling domains were defined with horizontal grid increment of 24 km (DO1; mesh size of 185 × 125) and 6 km (DO2; mesh size of 181 × 173), as shown in Fig. 1a. In the vertical dimension, 28 unevenly spaced full sigma levels were specified for both domains, with the model top defined at 100 hPa, corresponding to an altitude sufficiently higher than the average height of convective clouds observed during the examined case studies. The average vertical grid spacing near the surface and the tropopause approximates 50–100 m and 1000–1500 m, respectively.

The WRF model offers a great variety of parameterizations for the microphysics (MP), the radiation, the planetary boundary and surface layer (PBL/SL), the land-surface energy budget and the cumulus convection. Short-wave and long-wave radiation processes were handled with the Dudhia (Dudhia, 1989) and RRTM (Mlawer et al., 1997) schemes, respectively, while the Noah land surface model (Chen and Dudhia, 2001) was selected for the representation of land-surface processes.

2.1.1. Parameterization of lightning

To enable the parameterization of lightning, the Grell–Devenyi (GD) ensemble scheme (Grell and Devenyi, 2002) was chosen for cumulus convection. Lightning was consequently parameterized in both modeling domains using the approach of Price and Rind (1992), recently introduced in the WRF model by Wong et al. (2013).

In the WRF-based version of the PR92 scheme (Wong et al., 2013), lightning is parameterized using the model-resolved cloud-top height. The latter is defined as the height of the uppermost model level where deep convection, parameterized through the GD ensemble scheme, is simulated to occur. To account for the resolution dependency of PR92, a "calibration factor" was applied, as suggested in Price and Rind (1994). The empirical equation of Prentice and Mackerras (1977), based on latitude, was employed for partitioning the total lightning flash density derived by PR92 into intra-cloud (IC) and cloud-to-ground (CG) lightning. Further details on the implementation of PR92 in WRF can be found in Wong et al. (2013).

2.1.2. Sensitivity experiments

Although lightning and precipitation are not necessarily interdependent, they both relate with similar atmospheric processes, including ice–graupel collisions. Therefore, it is understandable that the prediction of lightning will depend strongly on the simulation of precipitation (Wong et al., 2013). Considering this, several numerical experiments were conducted to identify the best combination of parameterizations for the PBL/SL and MP, as regards the simulation of precipitation. The examined PBL/SL parameterizations include (a) the Yonsei University (YSU) PBL scheme (Hong et al., 2006) coupled with the MM5 similarity (MM5) SL scheme (Zhang and Anthes, 1982), and (b) the Mellor–Yamada–Janjic (MYJ) PBL scheme (Janjic, 1994) coupled with the Eta similarity (ETA) SL scheme (Janjic, 1996, 2002). The examined MP parameterizations include (a) the Purdue–Lin scheme (PL; Lin et al., 1983), (b) the WRF single-moment 6-class scheme (WSM6; Hong and Lim, 2006), and (c) the Thompson scheme (THOM; Thompson et al., 2008). Table 1 summarizes the different combinations between the above parameterizations, which were tested during the first stage of the WRF implementation.

All WRF simulations were initialized at 1200 UTC using the $1^o \times 1^o$ spatial resolution and 6 h temporal resolution operational atmospheric analysis surface and upper air data of the National Centre for Environmental Predictions (NCEP). High-

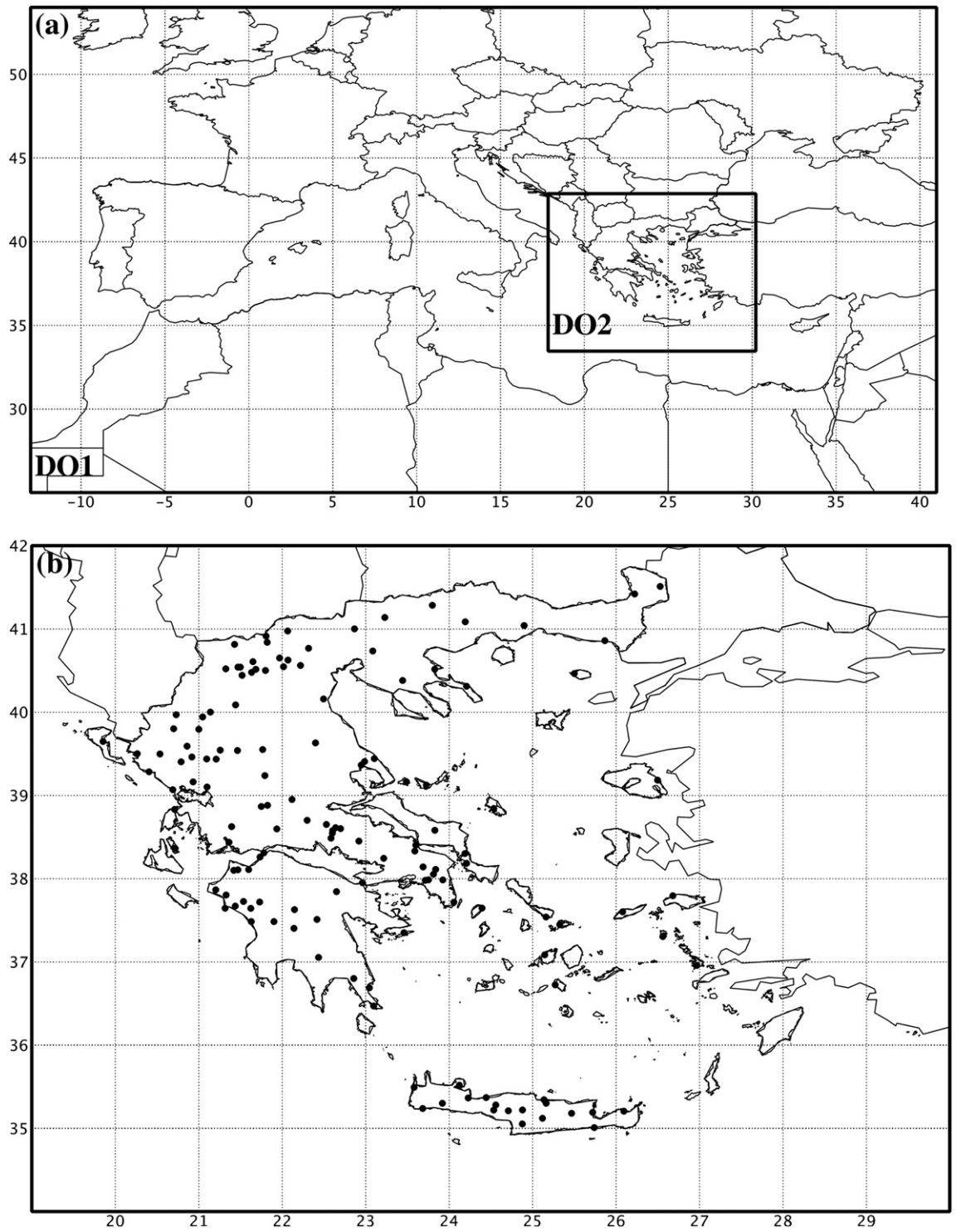

Fig. 1. (a) WRF modeling domains. (b) Locations of the 140 rain gauges (black circles) used for the verification of precipitation.

resolution ($0.085^o \times 0.085^o$) sea surface temperature analyses, provided by NCEP, were also used during the model initialization. The duration of the numerical simulations was set to 36 h, allowing for a 12 h spin-up period.

2.2. Case studies

For the purposes of the current study, ten single-day events in the period of the years 2010–2013 were selected. The key

Table 1
Summary of the different combinations of parameterizations for the planetary boundary and surface layer, and microphysics.

Configuration	PBL	SL	MP
SET1	YSU	MM5	PL
SET2	YSU	MM5	WSM6
SET3	YSU	MM5	THOM
SET4	MYJ	ETA	PL
SET5	MYJ	ETA	WSM6
SET6	MYJ	ETA	THOM

criterion for selecting the cases presented in Table 2 was the occurrence of widespread precipitation and lightning activity in Greece, while the specific meteorological conditions associated with each case were also taken into account. The selected case studies are classified into two groups. The first group contains the events that occurred during the warm period of year, spanning from May through September. The second group of events includes those that took place during the cold period of the year, spanning from October through April. This particular seasonal categorization has been based on similar previous studies (e.g. Kotroni and Lagouvardos, 2001; Mazarakis et al., 2009; Sindosi et al., 2012) and allows for examining model performance under different meteorological conditions associated with the occurrence of convection (e.g. thermally- versus dynamically-driven convection).

2.3. Verification procedure and data

At a first stage, six numerical experiments were conducted for each of the selected cases (Table 2). Each experiment was carried out using one of the configurations summarized in Table 1, resulting to 60 experiments in total. At a second stage, the configuration yielding the best overall model performance in terms of precipitation prediction was adopted for re-implementing the WRF model for each of the considered events, with the aim to evaluate the performance of the lightning prediction parameterization.

2.3.1. Precipitation

The 24 h accumulated precipitation from T0 + 12 to T0 + 36 at the 6 km modeling domain, was verified against observed precipitation from a network of 140 rain gauges, scattered within the Greek territory (Fig. 1b) and operated by the National Observatory of Athens. For the verification, the nine model grid points surrounding each rain gauge were first considered. The grid point with the closest value to the observed one was consequently selected as the predicted value. This selection approach was followed in order to avoid penalizing model performance due to small displacement of precipitation, which may originate from the adopted horizontal resolution.

Using the observed and predicted values, both qualitative and quantitative statistical measures were computed. For the qualitative evaluation, five 24 h accumulated rain thresholds were defined: above 1 mm, 2.5 mm, 5 mm, 10 mm and 20 mm. A 2×2 contingency table was used for evaluating the observed and model-resolved data for each of the thresholds and consequently computing the probability of detection (POD) and false alarm ratio (FAR) across the entire modeling domain. As regards the quantitative statistics, these include the quantity bias (QB) and the mean absolute error (MAE), both of which were determined for five rain ranges: 0.1–2.5 mm, 2.5–5 mm, 5–10 mm, 10–20 mm and > 20 mm.

Table 2
Summary of the 10 selected case studies, and associated observed maximum 24 h rainfall and synoptic meteorological conditions.

Date	Max. 24 h rainfall (mm)	Meteorological conditions
Warm period		
5 June 2010	>30 mm in 9 stations	Local convection
2 July 2010	>20 mm in 10 stations	Local convection
11 Sep 2010	>50 mm in 10 stations	Frontal system
21 Sep 2011	>20 mm in 12 stations	Frontal system
10 August 2012	>10 mm in 10 stations	Local convection
Cold period		
18 October 2010	>50 mm in 10 stations	Frontal system
12 January 2011	>20 mm in 14 stations	Longwave trough
6 February 2012	>50 mm in 11 stations	Frontal system
29 October 2012	>30 mm in 8 stations	Longwave trough
6 November 2013	>40 mm in 9 stations	Frontal system

2.3.2. Lightning

For the verification of lightning predictions, hourly measurements of CG lightning activity, aggregated to the 6 km horizontal resolution grid of WRF, were used. The observed lightning data were provided by the ground-based ZEUS network, which is a very low frequency (VLF) based lightning detection system. The detection efficiency of this network approximates 30%, while the location error is about 6.5 km. Further details on the ZEUS lightning network can be found in Kotroni and Lagouvardos (2008) and Lagouvardos et al. (2009).

The evaluation of the gridded observed and modeled lightning was conducted on a dichotomous decision basis (yes/no lightning occurrence). For this, the POD and FAR verification measures were computed, assuming a single lightning threshold: above 1 lightning count. This approach was followed since the primary aim of this study is to evaluate the WRF-based PR92 parameterization in terms of its suitability for real-time weather forecasting applications. In this context, the principal requirement is to assess the model's skill for correctly predicting the occurrence of lightning activity, both temporally and spatially, and not the lightning number.

3. Verification of precipitation

Fig. 2 summarizes the results obtained from the verification of the sensitivity experiments that were conducted, using the prescribed combinations of parameterizations for the PBL/SL and the MP (Table 1). POD, shown in Fig. 2a, measures the ability of the model to correctly predict the occurrence of precipitation events. In general, it can be seen that the differences between the scores of the different sets of configurations are small. Nevertheless, SETS4-6 are found to perform slightly better than SETS1-3, especially for the larger precipitation thresholds.

Fig. 2b depicts FAR, which is a verification score that quantifies the tendency of the model to falsely predict the occurrence of rain. Overall, all combinations yield rather small FAR values, lower than 0.40, which increase with increasing rain threshold. However, it is clear that SET6 provides the best overall performance, followed closely by SETS4-5.

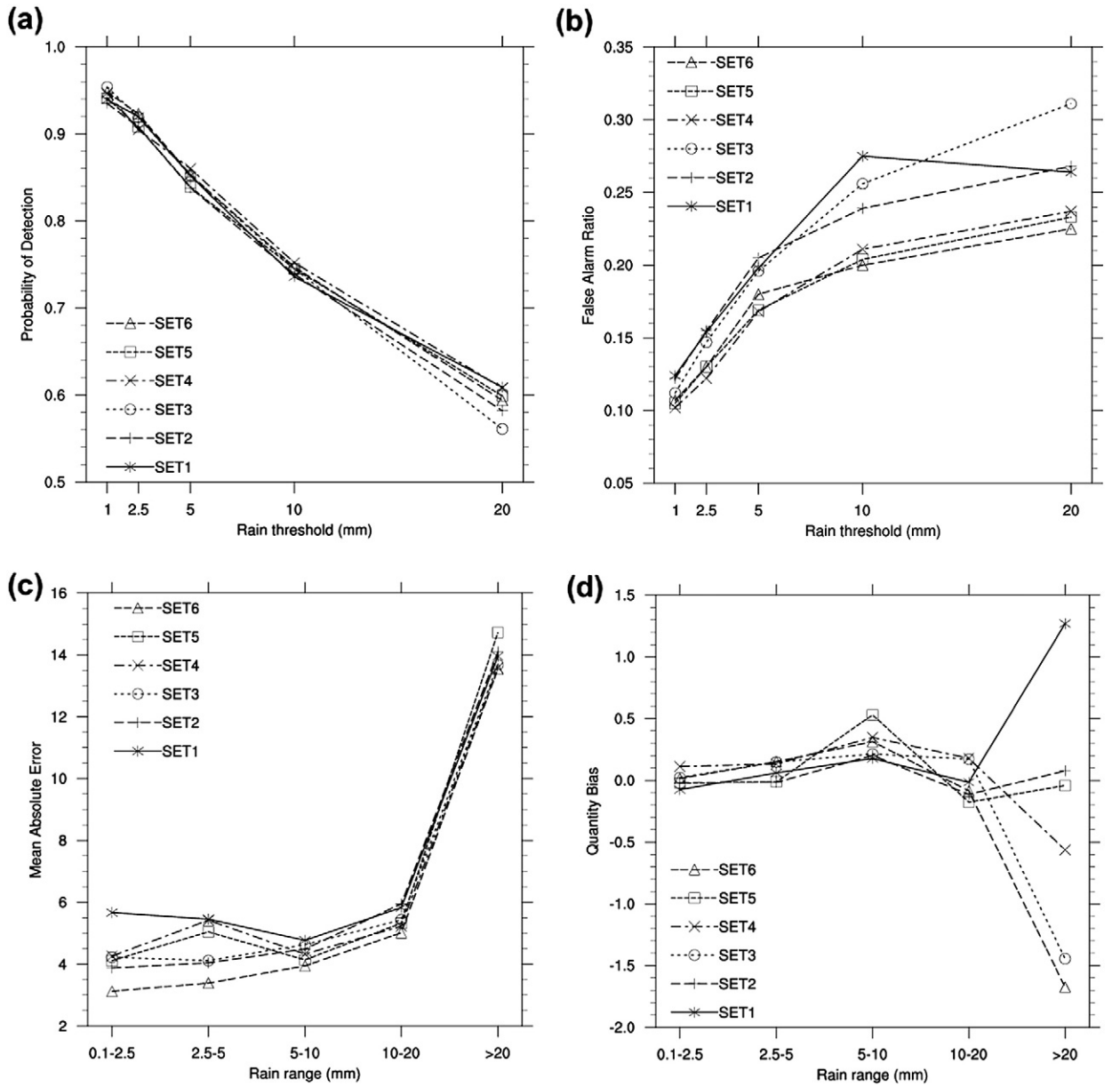

Fig. 2. (a) POD, (b) FAR, (c) MAE, and (d) QB for the 24 h WRF-simulated precipitation for the 6 different sets of physics configurations, averaged for the 10 selected cases.

For the quantitative verification of the simulated precipitation, MAE (Fig. 2c) and QB (Fig. 2d) are examined. The most striking feature is perhaps the significant increase of MAE for the heavy rain range (>20 mm), highlighting the inability of the model to reproduce heavy precipitation amounts, irrespective of the considered parameterizations' combination (Fig. 2c). This is in very good agreement with similar past studies, conducted over the same geographical area (i.e. eastern Mediterranean) and reporting increased model biases for large precipitation amounts (Efstathiou et al., 2013; Kotroni and Lagouvardos, 2001; Mazarakis et al., 2009). In general, SET6 shows the best overall MAE and QB, despite the fact that it also yields the largest underestimation for the >20 mm rain range (Fig. 2d). SET2 and SET5, for which QB values fluctuate around zero (Fig. 2d), are characterized by larger MAE values (Fig. 2c) than SET6 and thus, cannot be considered to be superior to it.

Putting all the above information together, it is rather clear that SET6 provides the best model simulations in terms of precipitation prediction. This is not very surprising since this particular set employs the THOM scheme for parameterizing microphysics, allowing for a more detailed representation of ice-phase processes than the PL and the WSM6 schemes. Better treatment of these processes is considered to be essential for a better simulation of precipitation (e.g. Efstathiou et al., 2012). The use of the MYJ PBL scheme also plays a role, primarily through the representation of the PBL top that is carried out

based on a prognostic equation for turbulent kinetic energy. Essentially, this allows for better representing atmospheric conditions that favor triggering convection. Consequently, SET6 was selected as the optimal configuration for re-implementing WRF in order to assess its skill with regards to lightning prediction.

4. Verification of lightning

Table 3 summarizes the POD and FAR scores that were computed for each of the selected events. It is easy to notice that WRF performs generally better during the warm than during the cold period of the year. This is primarily highlighted by the lower FAR scores, which yield an average warm period value of 0.56 (±0.11). For the cold period events, the average FAR score is significantly higher, equaling 0.71 (±0.11). On the other hand, the variation of POD between the examined cases is generally lower than the variation seen in FAR. This results to average warm/cold period values of about the same magnitude (0.88 ± 0.06 and 0.91 ± 0.04 for the warm and cold period events, respectively).

The high POD scores presented in Table 3 are desirable and indicate that the model succeeds in predicting the occurrence of lightning. However, FAR is also found to be high, showing rather unacceptable values that exceed ~0.50. This suggests that lightning activity is overpredicted. One potential cause could be the overestimation of the cloud-top height in the numerical simulations. Indeed, Wong et al. (2013) suggest applying a reduction of 2 km to reconcile the difference between the parameterized, through the GD ensemble scheme, cloud-top height and the value that it would have if explicitly resolved at a 20 dBZ reflectivity threshold. In the present study however, the application of the 2 km reduction did not result to improved model performance. This confirms Wong et al. (2013) who acknowledged that such a reduction might not be appropriate for capturing storm-to-storm variability, which is actually one of the goals of the present study.

4.1. Adaptation of the PR92 parameterization

The abovementioned results revealed the necessity to adapt PR92 by including model-simulated thermodynamical and microphysical variables as proxies for controlling the parameterization of lightning. The principal idea is to use certain variables as lightning predictors to develop a masking filter for the model-resolved lightning. Indeed, such an approach has been already used in past studies (e.g. Burrows et al., 2005; Zepka et al., 2014) for forecasting the probability of lightning.

In this study, several variables related to the microphysics and thermodynamics were examined as potential lightning predictors that could be used for the development of the masking filter. Based on literature review and common experience, threshold values were defined for each of the variables. Masking filters were consequently developed and applied to control the prediction of lightning through the WRF-based PR92 parameterization. The principal function of these filters is to prohibit lightning production when the pre-defined threshold values are not met.

Table 4 summarizes the verification results obtained after the implementation of the masking filters. For clarity, POD and FAR scores are averaged for all cases within each of the specified periods (i.e. warm or cold). The reported masking filters are based on: (a) the vertically integrated ice content (Q_{ice}) from the surface up to the model top (threshold value of 2 g), (b) the maximum vertical velocity (w_{max}) (threshold value of 0.25 m s^{-1}), (c) the convective available potential energy (CAPE) (threshold value of 250 J kg^{-1}), and (d) the combination of Q_{ice}, w_{max} and CAPE (threshold values as previously reported). It should be mentioned that several other variables (e.g. maximum ice/graupel flux, K-index, lifted index) and threshold values were also tested, but no better results than those reported in Table 4 were obtained.

Overall, it can be seen that all masking filters improve model performance for both the warm and the cold period events (Table 4). Among all variables, Q_{ice} and w_{max} appear to induce the largest improvements, while CAPE is found to perform more effectively for the warm period cases than for the cold ones. When combined together in a single masking filter, the overall performance of the model significantly improves. As shown in Table 4, FAR drops to 0.35 for the cold period and 0.28 for the warm period, corresponding to a reduction of about 50% compared to the scores obtained from the control simulations (i.e. no masking filter). On the other hand, POD is also found to decrease by about 20%, approximating 0.70 on average. This suggests that the implemented masking filter is successful in

Table 3
Summary of POD and FAR computed for the 10 selected events.

Case (date)	POD	FAR
Warm period		
5 June 2010	0.90	0.51
2 July 2010	0.88	0.44
11 September 2010	0.90	0.62
21 September 2011	0.95	0.72
10 August 2012	0.79	0.51
Cold period		
18 October 2010	0.92	0.74
12 January 2011	0.92	0.80
6 February 2012	0.94	0.77
29 October 2012	0.83	0.51
6 November 2013	0.92	0.72

Table 4
Summary of POD and FAR averaged for all cases in the warm and cold period, after the implementation of the different masking filters. For POD and FAR, values in parentheses refer to the standard deviation of the averages.

Masking filter (threshold value)	POD	FAR
Warm period		
No masking filter	0.88 (0.06)	0.56 (0.11)
Q_{ice} (2 g)	0.81 (0.07)	0.47 (0.08)
w_{max} (0.25 m s^{-1})	0.77 (0.06)	0.37 (0.08)
CAPE (250 J kg^{-1})	0.89 (0.04)	0.56 (0.11)
Q_{ice} (2 g)/w_{max} (0.25 m s^{-1})/ CAPE (250 J kg^{-1})	0.69 (0.08)	0.28 (0.08)
Cold period		
No masking filter	0.91 (0.04)	0.71 (0.11)
Q_{ice} (2 g)	0.85 (0.06)	0.67 (0.15)
w_{max} (0.25 m s^{-1})	0.78 (0.08)	0.49 (0.14)
CAPE (250 J kg^{-1})	0.88 (0.05)	0.63 (0.11)
Q_{ice} (2 g)/w_{max} (0.25 m s^{-1})/ CAPE (250 J kg^{-1})	0.71 (0.07)	0.35 (0.11)

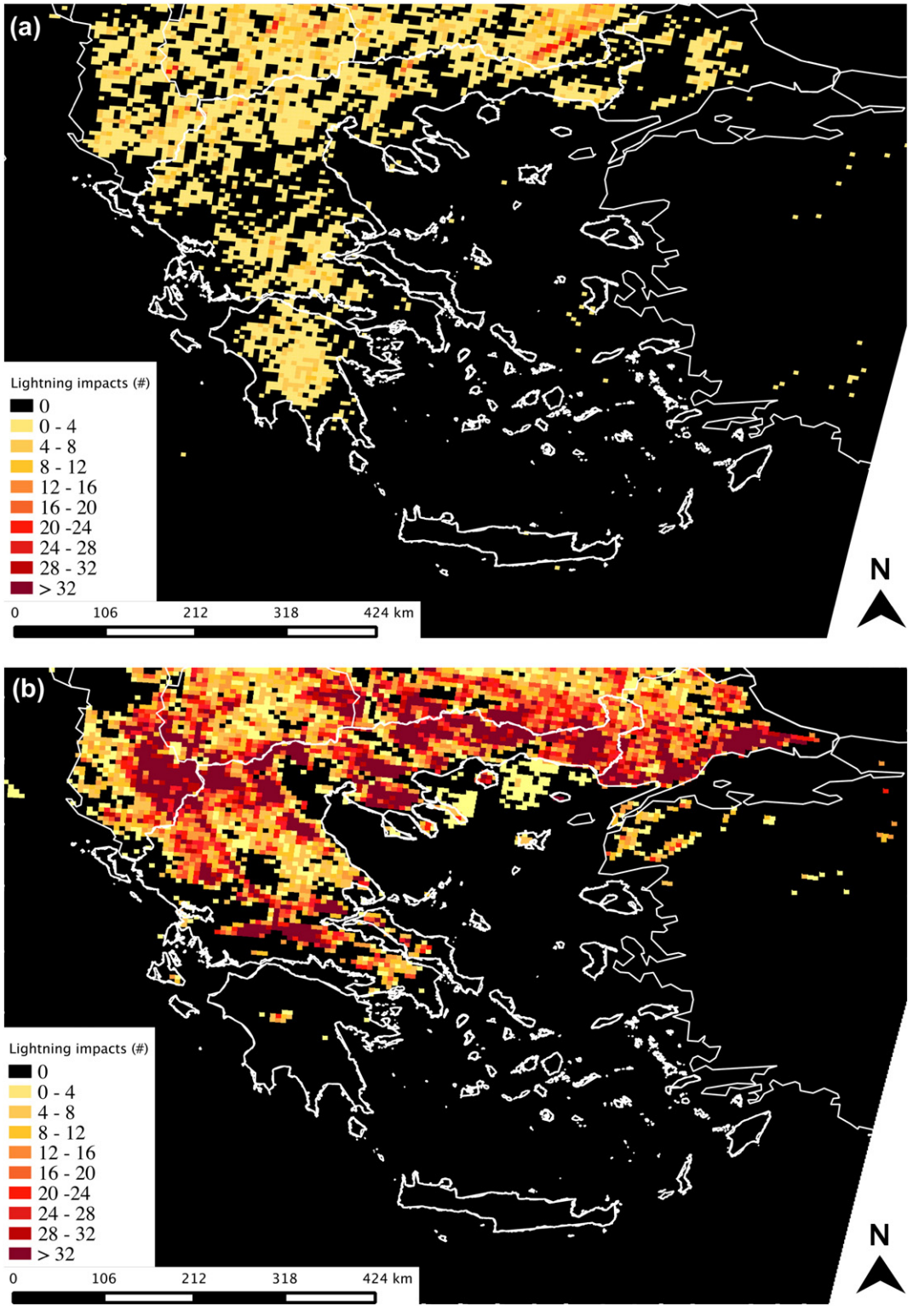

Fig. 3. (a) Observed, and (b) modeled 24 h accumulated lightning impacts for 2 July 2010, from 0000Z to 2400Z, aggregated to 6 km horizontal resolution.

restricting the model from falsely predicting lightning, while it does not significantly restrict the model's ability in terms of correct lightning predictions.

The results presented in Table 4 highlight the necessity for adapting the PR92 parameterization, especially when used for real-time weather forecasting applications. Indeed,

the significant reduction of FAR indicates that cloud-top height alone, upon which PR92 is based, is inadequate for determining whether convection is sufficient to produce lightning. The exploitation of other variables as proxies for evaluating the potential of model-resolved convection to produce lightning has proven to improve the overall model performance.

At this juncture of discussion, one could argue on the effectiveness of the proposed masking filters. Such an argument could be primarily based on the increase of uncertainty, induced due to the introduction of multiple model-simulated variables in the prediction of lightning (Barthe et al., 2010). Indeed, uncertainty increases and this could justify the reduction of POD scores along with the reduction seen in FAR. However, the restriction of the model's false alarms is found to be more profound than that of the reduction of POD. Further, the variables used in the masking filters enhance the physical foundation of lightning prediction. For instance, the presence of ice in the atmosphere is a requirement for lightning to occur, which is not included in the WRF-based PR92 parameterization. Vertical velocity and CAPE are also two important variables to consider for lightning production.

At this point it should be noted that the WRF-based PR92 parameterization of lightning offers the choice to either use the cloud-top height or the vertical velocity. The maximum vertical velocity has not been used for parameterizing lightning due to the adopted horizontal resolution (i.e. 6 km) that did not allow for explicitly resolving vertical convective motions.

4.2. Example case studies

Two example case studies, one for the warm and one for the cold period, are presented to enhance the analysis of model performance in terms of lightning prediction. For both events, the masking filter combining Q_{ice}, w_{max} and CAPE has been used. The presented lightning data, for both the model-predicted and observed datasets, refer to CG lightning. No adjustment is implemented on the observed lightning to account for the detection efficiency for ZEUS, while the WRF-simulated lightning data refer to the aggregated lightning flash counts from T0 + 12 through T0 + 36, where T0 is the initialization time of the simulations.

4.2.1. Warm period event: 2 July 2010

The event of 2 July 2010 is a typical example of summertime convection taking place over the major part of continental Greece during midday hours. As such, it can be considered to be an ideal case for examining the performance of WRF under convective conditions.

Fig. 3 presents the 24 h accumulated observed and modeled lightning impacts, aggregated to the 6 km horizontal resolution

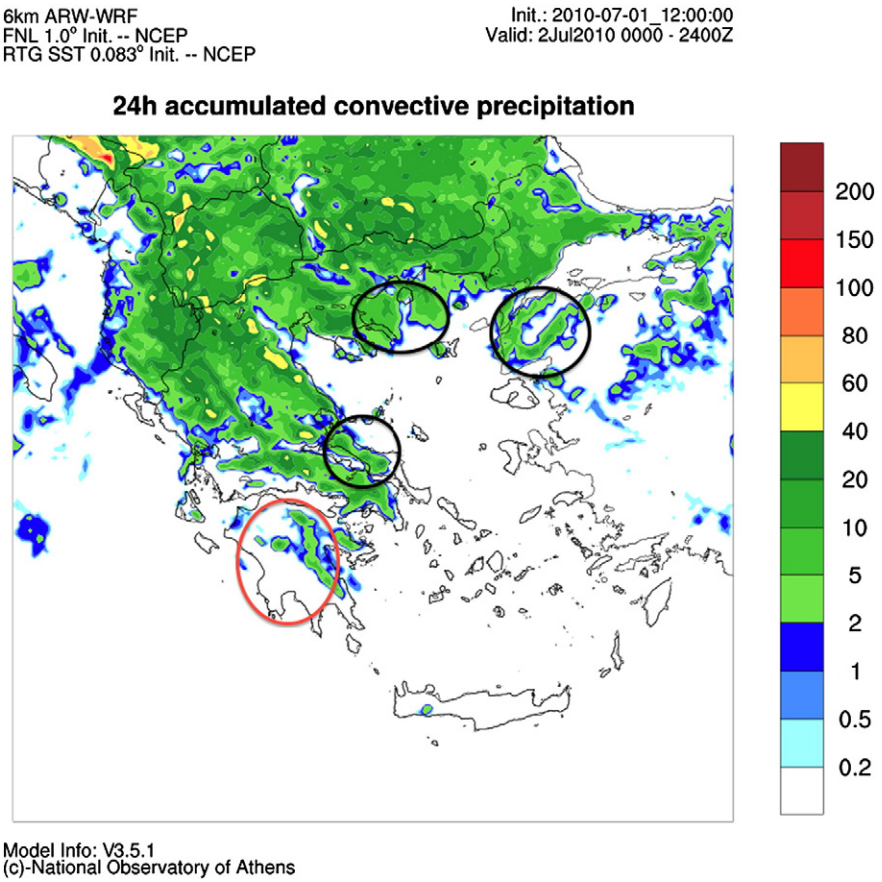

Fig. 4. Modeled 24 h accumulated convective precipitation for 2 July 2010.

WRF grid. Clearly, the model is capable of reproducing the key spatial features of lightning activity. In agreement with observations (Fig. 3a), widespread lightning is simulated to primarily occur over land (Fig. 3b). In particular, WRF successfully simulated lightning activity to be more compact over the northern parts of Greece than over the southern regions. However, it also failed to capture the occurrence of widespread lightning in southwest Greece. Comparing Fig. 3a and b, one could also notice the tendency of the model to overestimate the number of lightning impacts. This could be attributed, at least partially, to the detection efficiency of the Zeus lightning detection system that approximates 30% (Kotroni and Lagouvardos, 2008). Moreover, as already stated in Section 2.1.1, an empirical equation (Prentice and Mackerras, 1977) was employed for partitioning the total lightning flash density derived by PR92 into IC and CG lightning. This empirical equation only depends on latitude, and might be correct for climatological studies, while in our case, which is event based, this selection might also explain part of the differences between the modeled and observed number of lightning impacts.

In an attempt to shed more light on model performance, Fig. 4 presents the 24 h accumulated convective precipitation. Clearly, the spatial pattern of convective precipitation follows closely the spatial pattern of modeled lightning activity (Fig. 3b). In particular, it now becomes clear that the previously reported inability of the model to reproduce lightning over southwest Greece (Fig. 4; red circle) is directly associated with bad representation of convection over this area. The latter is also responsible for false prediction of lightning over certain regions of the study area, as highlighted in Fig. 4 with the black circles.

For real-time weather forecasting applications, an important factor to be taken into consideration is the ability of the model to capture the temporal distribution of lightning occurrence. For this, the hourly number of model grid points in domain DO2 (Fig. 1a) with observed and simulated lightning activity (i.e. at least one lightning impact) was computed. Results indicate that the daily evolution of lightning activity over Greece during the examined event was simulated reasonably well (Fig. 5). Although it is evident that WRF overpredicted lightning, showing grid points with at least one lightning impact throughout the entire event, the shape of the daily evolution of lightning activity was successfully reproduced. Indeed, both observations (Fig. 5a) and model results (Fig. 5b) indicate that widespread lightning was initiated in late morning (0700Z–0800Z), peaking during midday hours (1000Z–1300Z) and decreasing in the afternoon.

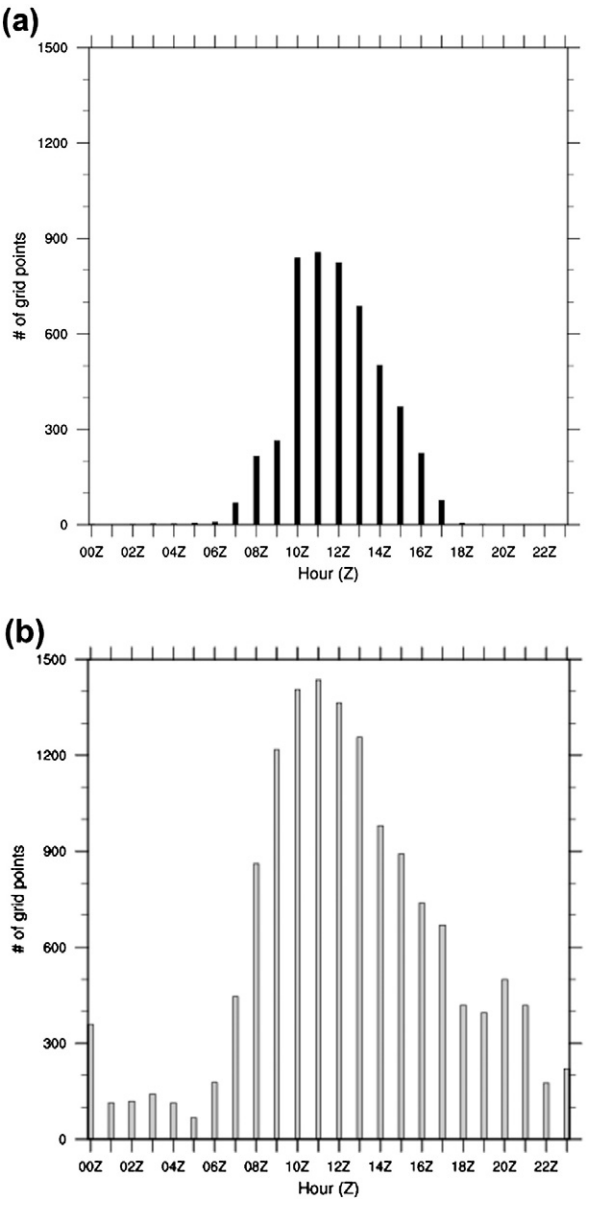

Fig. 5. Hourly evolution of (a) observed, and (b) simulated number of model grid points (D02; 6 × 6 km) affected by lightning on 2 July 2010.

4.2.2. Cold period event: 6 February 2012

The selected cold period event is a typical example of convection occurring during the approach of a low-pressure system from the southwest, associated with the development of a cold upper-air longwave trough. Therefore, it is thought to be a good example for analyzing model performance under conditions of dynamic instability that frequently occurs in winter.

WRF is found to reproduce reasonably well the spatial variability of lighting activity on 6 February 2012, as shown in Fig. 6. In particular, lightning was successfully simulated to occur across a southwest–northeast axis crossing Greece, associated with the movement of the low-pressure system that affected the study area. Further, the region of compact lightning activity at the southwest boundary of the domain was successfully captured, as well as the absence of lightning over the northern parts of the country. Similar to the warm period case, WRF seems to overestimate the number of lightning impacts. However, part of this overestimation should be attributed to the restricted detection efficiency of the Zeus lightning detection network, and/or the empirical partitioning of total forecasted lightning, as previously noted.

The spatial pattern of the 24 h accumulated convective precipitation (Fig. 7) is found to be in reasonable agreement with the spatial pattern of modeled lightning activity (Fig. 6b). As seen in Figs. 7 and 6b, there is close relation between the

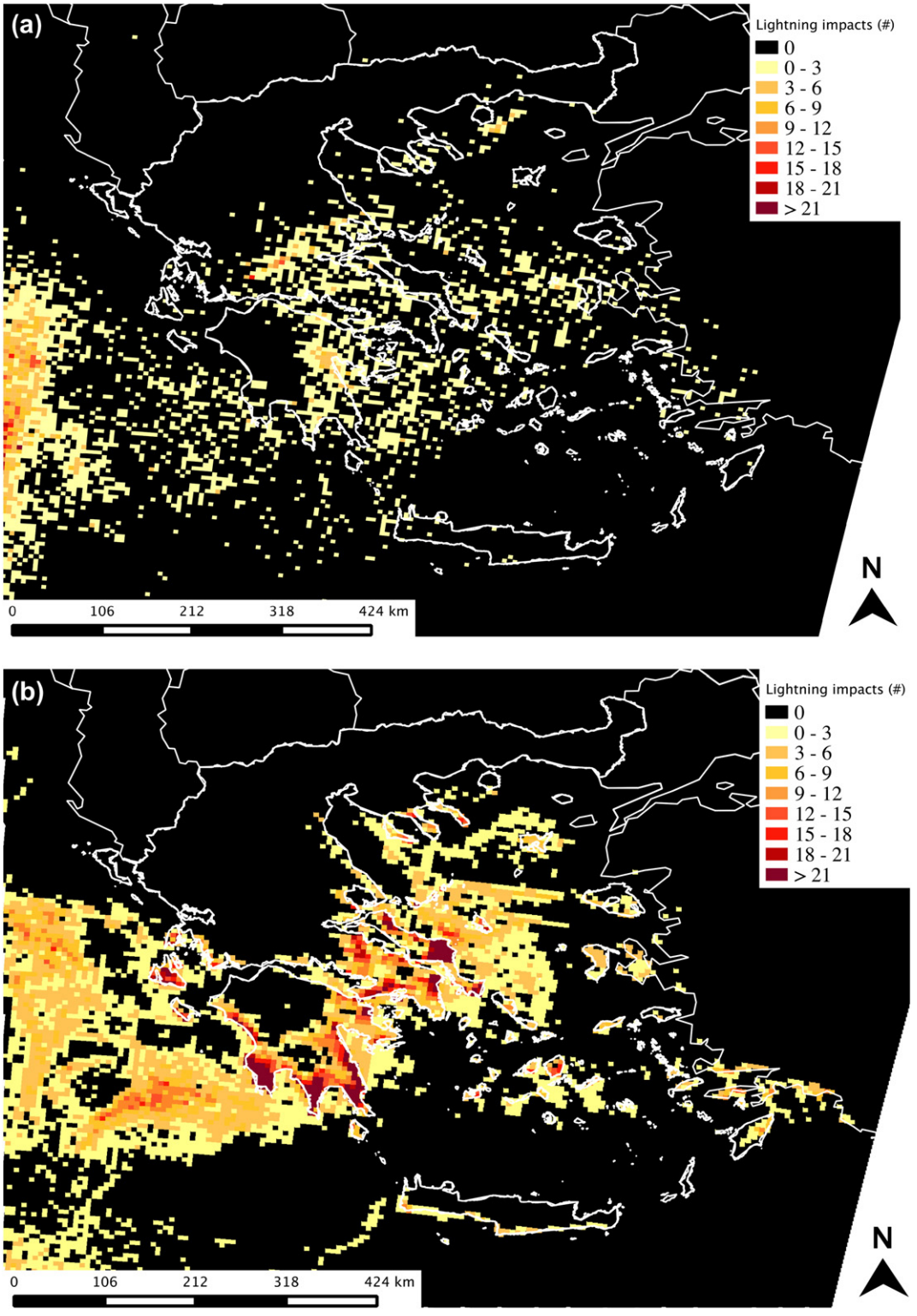

Fig. 6. (a) Observed, and (b) modeled 24 h accumulated lightning impacts for 6 February 2012, from 0000Z to 2400Z, aggregated to 6 km horizontal resolution.

regions of the highest convective precipitation and most intense modeled lightning activity (Fig. 7; black circles), also present in observations (Fig. 6a). However, the previously discussed bad representation of convection can be also found in this cold period case. For instance, the red circles in Fig. 7 highlight areas of the domain where, apparently, the model

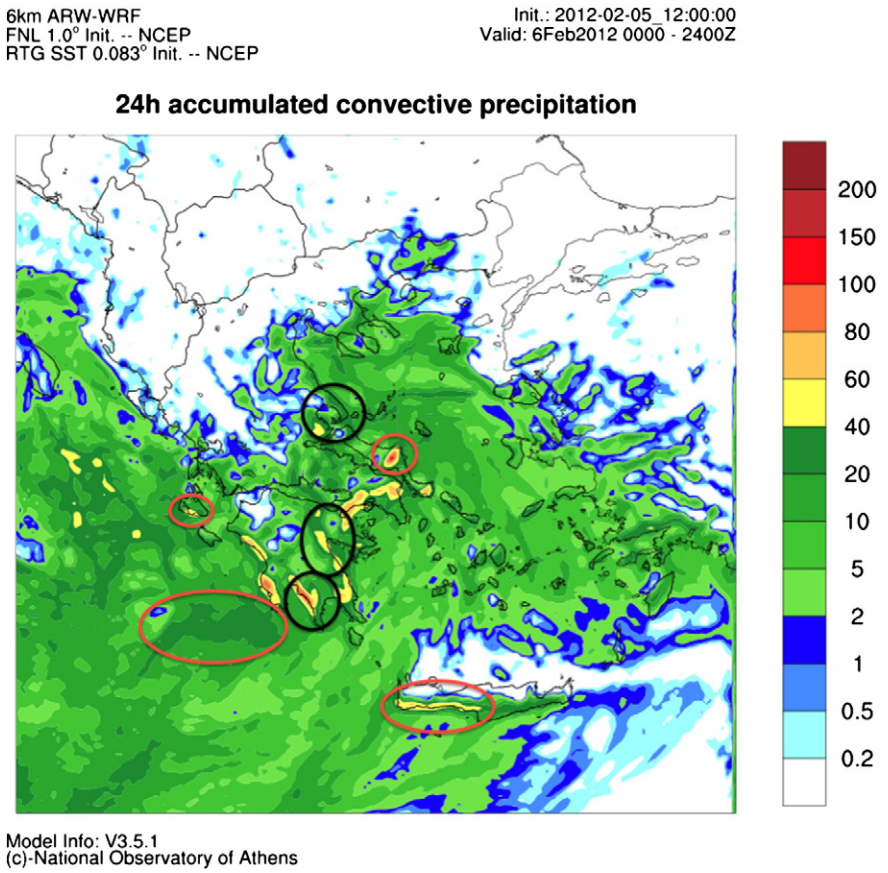

Fig. 7. Modeled 24 h accumulated convective precipitation for 6 February 2012.

simulated significant convective activity, resulting to falsely predicted lightning impacts.

With regard to the temporal variability, WRF shows adequacy in capturing the basic hourly march of lightning occurrence. As seen in Fig. 8, the model results agree with observations in that lightning activity started spreading across the study area in early morning hours (0400Z–0500Z), reaching a first peak at around noon (1000Z–1200Z). The decrease seen in observations (Fig. 8a) during the afternoon is not obvious in the numerical simulation (Fig. 8b), where a secondary peak is found (1400Z–1500Z). This could be attributed, at least partially, to the model's inability to correctly simulate the lifetime of the predicted storms, resulting in production of lightning for a longer time period than observed. Besides this, falsely predicted convection, capable of generating lightning, for certain regions of the modeling domain could also explain the above mentioned discrepancy. However, the persistence of lightning throughout the evening and until midnight is captured by the model.

5. Conclusions

The important implications of lightning on public safety, electrical infrastructures, aviation and upper tropospheric chemistry have driven significant progress in the development of predictive parameterizations for lightning. PR92 is one such parameterization that has been used in numerical models, primarily for supporting air quality applications. This lightning parameterization has been recently implemented in the NWP WRF model (Wong et al., 2013), allowing for its exploitation in the context of real-time weather forecasting activities.

In the present study, numerical simulations with the WRF model were conducted for 10 selected events in Greece, in order to examine the adequacy of PR92 as a tool for operational real-time lightning prediction. The conducted evaluation analysis focused primarily on the qualitative aspect of lightning prediction, exploiting observational data from ZEUS ground-based lightning detection network.

Results of this study suggest that the current implementation of PR92 in WRF requires proper adaptation to be suited for operational lightning prediction. The conducted numerical simulations revealed a clear tendency of the model to overpredict lightning activity, thus resulting to an unacceptable number of false alarms. This indicates that cloud-top height alone, upon which PR92 is based, is inadequate for determining whether the model-resolved convection is sufficient to produce lightning. Another possible cause for the overprediction of lightning could be the overestimation of cloud-top height. Additional numerical experiments conducted, reducing the cloud-top height as suggested by Wong et al. (2013), did not improve the model performance.

To tackle the critical issue of lightning overprediction, model-resolved microphysical and thermodynamical variables were used for developing masking filters with the aim to

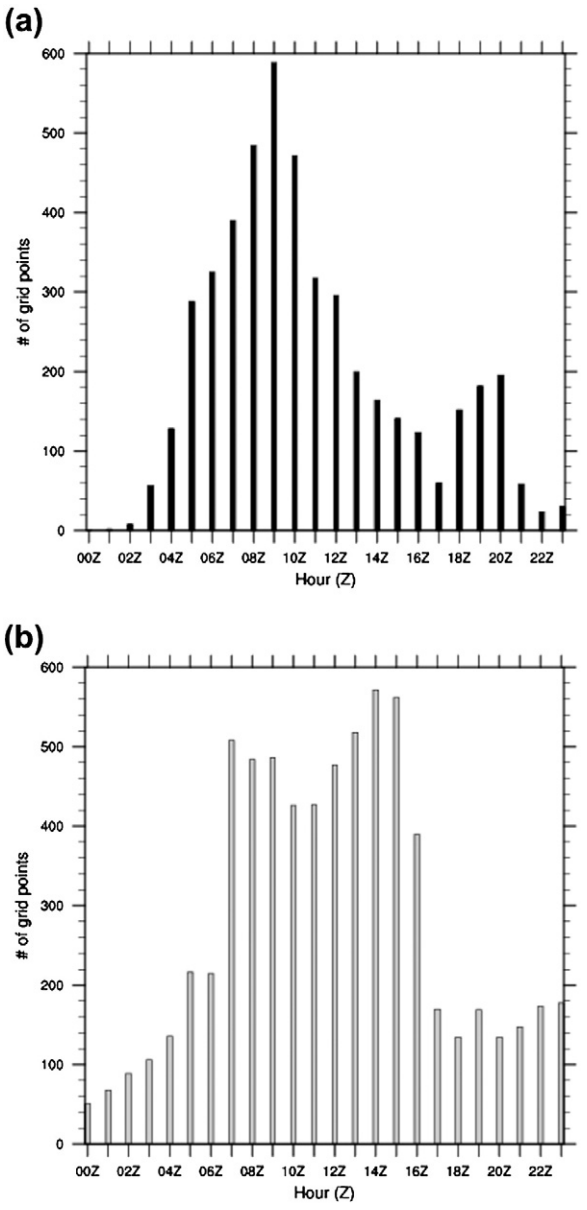

Fig. 8. Hourly evolution of (a) observed, and (b) simulated number of model grid points (D02; 6 × 6 km) affected by lightning on 6 February 2012.

control the production of lightning through PR92. This approach was motivated by previous studies, reporting on the correlation between lightning and storm parameters. It was found that the implementation of specific masking filters improves model performance, by restricting PR92 from overproducing lightning. In particular, the best performing masking filter was found to be the one combining the total column ice content, the maximum vertical velocity and the convective available potential energy. Together with the cloud-top height, the previously mentioned variables seem to be adequately successful in determining the capacity of model-resolved convection to produce lightning.

The adapted, through the masking filters, WRF-based PR92 lightning parameterization resulted to significantly improved overall model performance, characterized by generally low FAR and satisfactorily high POD scores. The numerical simulations were also quite successful in reproducing the key features of the spatiotemporal variability of lightning activity on an event-by-event basis. This was highlighted in the analysis of two example case studies, suggesting that although additional variables may increase uncertainty, they are still necessary to obtain more realistic lightning predictions.

The conducted analysis also revealed that the representation of convection in the model is an important factor for simulating lightning activity. It was found that the ability of WRF to correctly or falsely predict lightning is directly related to its ability to correctly or falsely predict convection to occur, respectively. For the particular region of the present study, this highlights the necessity of employing a CPS. However, this could be different for another region, depending also on the specified horizontal grid spacing. In this context, it is important to evaluate model performance, prior to deciding whether parameterized or explicitly resolved storm parameters will be used for lightning prediction.

Summarizing, the results of the present study provide strong evidence that PR92 should be considered to be a robust parameterization for real-time lightning prediction, given that the necessary adaptations are implemented. It is important to underline that the proposed adaptations may differ according to the considered study area. For instance, the storm parameters and/or the specified thresholds used for developing the masking filter, or even the need for such a filter, may be different for another region, depending also on the adopted horizontal grid resolution. For this, it would be of great interest for the future to extend the present study to other regions, where the characteristics of storm events and convection may deviate from those considered herein.

Acknowledgments

The authors acknowledge funding by the European Union (European Social Fund) and National Resources under the "ARISTEIA II" action of the Operational Programme "Education and Lifelong Learning" in Greece, Project TALOS-3449.

References

Allen, D.J., Pickering, K.E., 2002. Evaluation of lightning flash rate parameterizations for use in a global chemical transport model. J. Geophys. Res. 107, D02066.

Allen, D.J., Pickering, K.E., Duncan, B., Damon, M., 2010. Impact of lightning NO emissions on North American photochemistry as determined using the Global Modeling Initiative (GMI) model. J. Geophys. Res. 115, D14062.

Ashley, W.S., Gilson, C.W., 2009. A reassessment of U.S. lightning mortality. Bull. Am. Meteorol. Soc. 90, 1501–1518.

Barthe, C., Deirling, W., Barth, M.C., 2010. Estimation of total lightning from various storm parameters: a cloud-resolving model study. J. Geophys. Res. 115 (D24), D24202.

Biazar, A.P., McNider, R.T., 1995. Regional estimates of lightning production of nitrogen oxides. J. Geophys. Res. 100 (D11), 22861–22874.

Burrows, W.R., Price, C., Wilson, L.J., 2005. Warm season lightning probability prediction for Canada and the Northern United States. Weather Forecast. 20, 971–988.

Chen, F., Dudhia, J., 2001. Coupling an advanced land surface-hydrology model with the Penn State-NCAR MM5 modeling system. Part I: model implementation and sensitivity. Mon. Weather Rev. 129, 569–585.

Choi, Y., Wang, Y., Zeng, T., Martin, R.V., Kurosu, T.P., Chance, K., 2005. Evidence of lightning NO_x and convective transport of pollutants in satellite observations over North America. Geophys. Res. Lett. 32, L02805.

Cooper, O.R., Trainer, M., Thompson, A.M., Oltmans, S.J., Tarasick, D.W., Witte, J.C., Stohl, A., Eckhardt, S., Lelieveld, J., Newchurch, M.J., Johnson, B.J., Portmann, R.W., Kalnajs, L., Dubey, M.K., Leblanc, T., McDermid, I.S., Forbes, G., Wolfe, D., Carey-Smith, T., Morris, G.A., Lefer, B., Rapengluck, B., Joseph, E., Schmidlin, F., Meagher, J., Fehsenfeld, F.C., Keating, T.J., Van Curen, R.A., Minschwaner, K., 2007. Evidence for a recurring Eastern North America upper tropospheric ozone maximum during summer. J. Geophys. Res. 112, D23304.

Deierling, W., Petersen, W.A., 2008. Total lightning activity as an indicator of updraft characteristics. J. Geophys. Res. 113, D16210.

Drobyshev, I., Flannigan, M.D., Bergeron, Y., Girardin, M.P., Suran, B., 2010. Variation in local weather explains differences in fire regimes within a Quebec south-eastern boreal forest landscape. Int. J. Wildland Fire 19 (8), 1073–1082.

Dudhia, J., 1989. Numerical study of convection observed during the winter monsoon experiment using a mesoscale two-dimensional model. J. Atmos. Sci. 46, 3077–3107.

Efstathiou, G.A., Zoumakis, N.M., Melas, D., Kassomenos, P., 2012. Impact of precipitating ice on the simulation of a heavy rainfall event with advanced research WRF using two bulk microphysical schemes. Asia-Pac. J. Atmos. Sci. 48 (4), 357–368.

Efstathiou, G.A., Zoumakis, N.M., Melas, D., Lolis, C.J., Kassomenos, P., 2013. Sensitivity of WRF to boundary layer parameterizations in simulating a heavy rainfall event using different microphysical schemes: Effect on large-scale processes. Atmos. Res. 132, 125–143.

Elsom, D.M., 2000. Deaths and injuries caused by lightning in the United Kingdom: analysis of two databases. Atmos. Res. 56, 325–334.

Grell, G.A., Devenyi, D., 2002. A generalized approach to parameterizing convection combining ensemble and data assimilation techniques. Geophys. Res. Lett. 29, L15311.

Hong, S.Y., Lim, J.J.O., 2006. The WRF single-moment 6-class microphysics scheme (WSM6). J. Korean Meteorol. Soc. 42, 129–151.

Hong, S.Y., Noh, Y., Dudhia, J., 2006. A new vertical diffusion package with an explicit treatment of entrainment processes. Mon. Weather Rev. 134, 2318–2341.

Hudman, R.C., Jacob, D.J., Turquety, S., Leibensperger, E.M., Murray, L.T., Wu, S., Gilliland, A.B., Avery, M., Bertram, T.H., Brune, W., Cohen, R.C., Dibb, J.E., Flocke, F.M., Fried, A., Holloway, J., Neuman, J.A., Orville, R., Perring, A., Ren, X., Sachse, G.W., Singh, H.B., Swanson, A., Woodridge, P.J., 2007. Surface and lightning sources of nitrogen oxides over the United States: magnitudes, chemical evolution, and outflow. J. Geophys. Res. 112 (D12). http://dx.doi.org/10.1029/2006JD007912.

Janjic, Z.I., 1994. The step-mountain eta coordinate model: further developments of the convection, viscous sublayer and turbulence closure schemes. Mon. Weather Rev. 122, 927–945.

Janjic, Z.I., 1996. The surface layer in the NCEP Eta model. Eleventh Conference on Numerical Weather Prediction, Norfolk, VA, 19–23 August, Amer. Meteor. Soc., Boston, MA, pp. 354–355.

Janjic, Z.I., 2002. Nonsingular implementation of the Mellor–Yamada level 2.5 scheme in the NCEP meso model. NCEP Office Note No. 437 (61 pp.).

Kotroni, V., Lagouvardos, K., 2001. Precipitation forecast skill of different convective parameterization and microphysical schemes: application for the cold season over Greece. Geophys. Res. Lett. 28, 1977–1980.

Kotroni, V., Lagouvardos, K., 2008. Lightning occurrence in relation with elevation, terrain slope and vegetation cover in the Mediterranean. J. Geophys. Res.-Atmos. 113, D21118.

Lagouvardos, K., Kotroni, V., Betz, H.D., Schmidt, K., 2009. A comparison of lighting data provided by ZEUS and LINET networks over Western Europe. Nat. Hazards Earth Syst. Sci. 9, 1713–1717.

Lin, Y.L., Farley, R.D., Orville, H.D., 1983. Bulk parameterization of the snow field in a cloud model. J. Clim. Appl. Meteorol. 22, 1065–1092.

Liu, W., Wang, S., Zhou, Y., Wang, L., Zhang, M., 2010. Lightning-caused forest fires risk assessment based on historical fires events in Daxingan Mountains of China. Disaster Adv. 3 (4), 143–147.

Lynn, B.H., Yair, Y., Price, C., Kelman, G., Clark, A.J., 2012. Predicting cloud-to-ground and intracloud lightning in weather forecast models. Weather Forecast. 27, 1470–1488.

Mazarakis, N., Kotroni, V., Lagouvardos, K., Argiriou, A.A., 2009. The sensitivity of numerical forecasts to convective parameterization during the warm period and the use of lightning data as an indicator for convective occurrence. Atmos. Res. 94, 704–714.

McCaul, E.W., Goodman, S.J., LaCasse, K.M., Cecil, D.J., 2009. Forecasting lightning threat using cloud-resolving model simulations. Weather Forecast. 24, 709–729.

Mlawer, E.J., Taubman, S.J., Brown, P.D., Iacono, M.J., Clough, S.A., 1997. Radiative transfer for inhomogeneous atmosphere: RRTM, a validated correlated-k model for the longwave. J. Geophys. Res. 102 (D14), 16663–16682.

Papagiannaki, K., Lagouvardos, K., Kotroni, V., 2013. A database of high-impact weather events in Greece: a descriptive impact analysis for the period 2001–2011. Nat. Hazards Earth Syst. Sci. 13, 727–736.

Petersen, W.A., Christian, H.J., Rutledge, S.A., 2005. TRMM observations of the global relationship between ice water content and lightning. Geophys. Res. Lett. 32, L14819.

Peterson, D., Wang, J., Ichoku, C., Remer, L.A., 2010. Effects of lightning and other meteorological factors on fire activity in the North American boreal forest: implications for fire weather forecasting. Atmos. Chem. Phys. 10 (14), 6873–6888.

Pickering, K.E., Thompson, A.M., Scala, J.R., Tao, W.K., Dickerson, R.R., Simpson, J., 1992. Free tropospheric ozone production following entrainment of urban plumes into deep convection. J. Geophys. Res. 97 (D16), 17985–18000.

Prentice, S.A., Mackerras, D., 1977. The ratio of cloud to cloud–ground lightning flashes in thunderstorms. J. Appl. Meteorol. 16, 545–549.

Price, C., Rind, D., 1992. A simple lightning parameterization for calculating global lightning distributions. J. Geophys. Res. 97 (D9), 9919–9933.

Price, C., Rind, D., 1994. Modeling global lightning distributions in a general circulation model. Mon. Weather Rev. 112, 1930–1939.

Ryu, J.H., Jenkins, G.S., 2005. Lightning-tropospheric ozone connections: EOF analysis of TCO and lightning data. Atmos. Environ. 39 (32), 5799–5805.

Sindosi, O.A., Bartzokas, A., Kotroni, V., Lagouvardos, K., 2012. Verification of precipitation forecasts of MM5 model over Epirus, NW Greece, for various convective parameterization schemes. Nat. Hazards Earth Syst. Sci. 12, 1393–1405.

Skamarock, W.C., Klemp, J.B., Dudhia, J., Gill, D.O., Barker, D.M., Duda, M.G., Huang, X.Y., Wang, W., Powers, J.G., 2008. A description of the Advanced Research WRF version 3. NCAR Technical Note, NCAR/TN-475+STR, Mesoscale and Microscale Meteorology Division, National Centre for Atmospheric Research, Boulder, Colorado, USA.

Stockwell, D.Z., Giannakopoulos, C., Plantevin, P.H., Carver, G.D., Chipperfield, M.P., Law, K.S., Pyle, J.A., Shallcross, D.E., Wang, K.Y., 1999. Modeling NO_x from lightning and its impact on global chemical fields. Atmos. Environ. 33, 4477–4493.

Thompson, G., Field, P.R., Rasmussen, R.M., Hall, W.D., 2008. Explicit forecasts of winter precipitation using an improved bulk microphysics scheme. Part II: implementation of a new snow parameterization. Mon. Weather Rev. 136, 5095–5115.

Wong, J., Barth, M.C., Noone, D., 2013. Evaluating a lighting parameterization based on cloud-top height for mesoscale numerical model simulations. Geosci. Model Dev. 6, 429–443.

Yair, Y., Lynn, B., Price, C., Kotroni, V., Lagouvardos, K., Morin, E., Mugnai, A., Llasat, M.C., 2010. Predicting the potential for lightning activity in Mediterranean storms based on the Weather Research and Forecasting (WRF) model dynamic and microphysical fields. J. Geophys. Res. — Atmos. 115, D04205.

Zepka, G.S., Pinto Jr., O., Saraiva, A.C.V., 2014. Lightning forecasting in southeastern Brazil using the WRF model. Atmos. Res. 135–136, 344–362.

Zhang, D.L., Anthes, R.A., 1982. A high-resolution model of the planetary boundary layer — sensitivity tests and comparisons with SESAME-79 data. J. Appl. Meteorol. 21, 1594–1609.

Zhao, C., Wang, Y., Choi, Y., Zeng, T., 2009. Summertime impact of convective transport and lightning NO_x production over North America: modeling dependence on meteorological simulations. Atmos. Chem. Phys. 9, 4315–4327.